

# Studies on lanthanide complexes of the tripodal ligand bis(2-benzimidazolymethyl)(2-pyridylmethyl)amine. Crystal structures and luminescence properties †

Xiao-Ping Yang,<sup>ab</sup> Cheng-Yong Su,<sup>\*a</sup> Bei-Sheng Kang,<sup>\*a</sup> Xiao-Long Feng,<sup>a</sup> Wang-Leng Xiao<sup>c</sup> and Han-Qin Liu<sup>a</sup>

<sup>a</sup> School of Chemistry and Chemical Engineering, Zhongshan University, Guangzhou 510275, P. R. China. E-mail: cessay@zsu.edu.cn

<sup>b</sup> State Key Laboratory of Rare Earth Materials Chemistry and Applications, Peking University, Beijing 100871, P. R. China

<sup>c</sup> Institute of Laser and Spectroscopy, Zhongshan University, Guangzhou 510275, P. R. China

Received 4th May 2000, Accepted 27th July 2000

First published as an Advance Article on the web 5th September 2000

A new unsymmetric tripodal ligand bis(2-benzimidazolymethyl)(2-pyridylmethyl)amine (L) bearing two kinds of chromophores benzimidazole and pyridine has been synthesized, and two series of lanthanide(III) complexes [LnL(NO<sub>3</sub>)<sub>3</sub>]·C<sub>2</sub>H<sub>5</sub>OH (Ln = La, Sm, Eu, Gd, Tb or Tm) and [LnLCl<sub>3</sub>(H<sub>2</sub>O)]·C<sub>2</sub>H<sub>5</sub>OH (Ln = La, Sm, Eu, Tb or Ho) have been characterized by elemental analyses, FAB mass spectra, <sup>1</sup>H NMR, conductivity measurements, and IR spectra. The crystal and molecular structures of the three complexes [SmL(NO<sub>3</sub>)<sub>3</sub>]·C<sub>2</sub>H<sub>5</sub>OH **1**, [GdL(NO<sub>3</sub>)<sub>3</sub>]·C<sub>2</sub>H<sub>5</sub>OH **2**, and [SmLCl<sub>3</sub>(H<sub>2</sub>O)]·C<sub>2</sub>H<sub>5</sub>OH **3** have been determined by X-ray diffraction analysis. **1** and **2** are isomorphous with the central metal ion co-ordinated by the four nitrogen atoms of the ligand and six oxygen atoms of three chelating nitrate groups. In complex **3**, besides the four nitrogen atoms of the ligand and three chlorine atoms, there is one H<sub>2</sub>O molecule co-ordinated. Conductivity studies on the [LnL(NO<sub>3</sub>)<sub>3</sub>]·C<sub>2</sub>H<sub>5</sub>OH complexes in methanol showed that two of the nitrate anions dissociate to give 2:1 electrolytes. Comparison of the emission lifetimes of the Eu<sup>3+</sup> and Tb<sup>3+</sup> complexes in CH<sub>3</sub>OH and CD<sub>3</sub>OD gives the average value for *q*, the number of co-ordinated methanol molecules, of 3.4, suggesting the formation of species [LnL(NO<sub>3</sub>)(CH<sub>3</sub>OH)<sub>3</sub>][NO<sub>3</sub>]<sub>2</sub>. The emission quantum yields of the nitrate-co-ordinated series are substantially higher than those of the chloride series, as shown by luminescence studies in MeCN.

## Introduction

There have been vigorous studies on the chemistry of multi-dentate ligands with lanthanide(III) ions in the past decade. Much of this has been spurred by their potential uses as supramolecular devices,<sup>1–3</sup> fluorescent sensors, or luminescent probes.<sup>4–7</sup> In order to obtain strongly luminescent complexes, the chromophoric ligands which chelate to the lanthanide metals should be able (i) to absorb energy and transfer it efficiently to the central metal and (ii) to encapsulate and protect the lanthanide ion from the solvent molecules.<sup>1</sup> For these purposes, macrocyclic, macrobicyclic (cryptand) and podand-type ligands have extensively been used.<sup>8–11</sup>

Work on the applications of lanthanide complexes as contrast agents for magnetic resonance imaging (MRI), luminescent stains of fluoroimmunoassays, and catalysts for the selective cleavage of RNA and DNA requires close and tunable control of the co-ordination sphere to enhance specific structural and electronic properties.<sup>12–14</sup> As contrasting agents, the tripodal ligands derived from Schiff-base condensation with tris(2-aminoethyl)amine (tren) have attracted much attention.<sup>15–17</sup> With three suitably designed arms, the tripodal ligands could provide hosts for the lanthanide ions and well encapsulate them, and by deliberate incorporation of appropriate multiple absorption groups suitable for energy transfer they could be used to develop strongly luminescent lanthanide

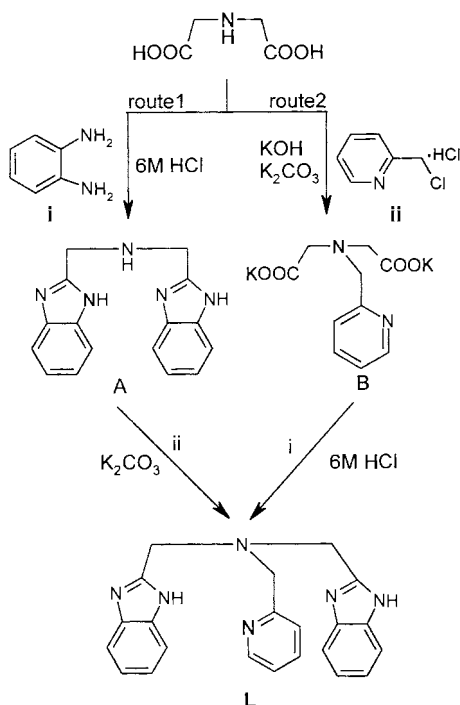
complexes.<sup>1,3</sup> Based on the inherent character of the benzimidazole group which allows easy derivation and potentially strong π–π stacking interaction to form supramolecular structures,<sup>18,19</sup> we have investigated lanthanide complexes with tripodal ligands incorporating benzimidazole rings.<sup>20–22</sup> The luminescent lanthanide complexes of a symmetric tripodal N-donor ligand tris(benzimidazol-2-ylmethyl)amine (ntb) have been prepared, indicating that such ligands with benzimidazole groups are good candidates to obtain high luminescence.<sup>20</sup> In an effort to explore these kind of complexes in more detail to inspect the ligand-to-metal energy transfer efficiency, herein we describe a new unsymmetric tripodal ligand bis(2-benzimidazolymethyl)-(2-pyridylmethyl)amine (L, Scheme 1) bearing two kinds of chromophores, benzimidazole and pyridine, and two series of its lanthanide complexes.

## Experimental

### General comments

Hydrated lanthanide nitrates and chlorides were prepared by dissolving the corresponding oxides (99.1%) in 50% nitric acid and 40% hydrochloric acid, respectively. *o*-Phenylenediamine, iminodiacetic acid and 2-pyridylmethyl chloride hydrochloride were obtained from Aldrich and used without further purification. Elemental analyses (C, H, N) were carried out on a Varian EL elemental analyser. <sup>1</sup>H NMR spectra were recorded on a Varian INOVA 500 spectrometer, UV spectra on a SHIMADZU UV-2501PC spectrophotometer, infrared spectra from 4000 to 400 cm<sup>-1</sup> on a Bruker EQINOX 55 FT-IR and fast atom bombardment (FAB) mass spectra on a VG ZAB-HS

† Electronic supplementary information (ESI) available: hydrogen bonded network in complex **1**, <sup>1</sup>H NMR spectra, decay curves and selected bond angles for **1**–**3**. See <http://www.rsc.org/suppdata/dt/b003566/>



Scheme 1 Synthetic routes for the preparation of the ligand L.

instrument. Conductivity measurements were carried out with a DDS-11 conductivity bridge for  $10^{-3}$  mol  $\text{dm}^{-3}$  solutions in  $\text{CH}_3\text{CN}$  and  $\text{CH}_3\text{OH}$ .

#### Synthesis of ligand

The ligand bis(2-benzimidazolylmethyl)(2-pyridylmethyl)amine (L) was prepared by the following synthetic routes.

**Method 1.** *Bis(2-benzimidazolylmethyl)amine*. Reaction was run according to ref. 23, and the compound obtained as a white solid, yield 29%.  $\delta_{\text{H}}$  ( $(\text{CD}_3)_2\text{SO}$ , 298 K) 4.01 (s, 4 H), 7.13 (m, 4 H) and 7.51 (m, 4 H).  $\tilde{\nu}_{\text{max}}/\text{cm}^{-1}$  3395 (br), 3184, 1616s, 1539, 1440, 1307 and 744s.

*Bis(2-benzimidazolylmethyl)(2-pyridylmethyl)amine (L)*. To a solution of bis(2-benzimidazolylmethyl)amine (2.77 g, 0.01 mol) in methanol (150 ml) was added  $\text{K}_2\text{CO}_3$  (2.00 g, 0.014 mol) and the mixture stirred and heated for 10 min. 2-Pyridylmethyl chloride hydrochloride (3.28 g, 0.02 mol) in 50 ml of methanol was added dropwise in 30 min and the resulting solution stirred and heated to reflux under nitrogen for 24 h. After filtration, the filtrate was reduced in volume at low pressure to leave a brown residue which was dissolved in 60 ml of  $\text{CHCl}_3$  and filtered. The filtrate was washed with 20 ml of 0.1 M NaOH solution three times and the  $\text{CHCl}_3$  removed at low pressure to leave a solid that was recrystallised from ethanol to give 0.56 g of product (15%).  $\tilde{\nu}_{\text{max}}/\text{cm}^{-1}$  3220 (br), 3145 (br), 3054, 1622, 1594, 1588, 1538, 1484, 1434s, 1350, 1272, 999 and 746s. FAB MS and elemental analysis data are summarized in Table 1.

**Method 2.** *Dipotassium N-(2-pyridylmethyl)iminodiacetate*. Iminodiacetic acid (2.66 g, 0.02 mol) was dissolved in an aqueous solution (20 ml) of KOH (2.24 g, 0.04 mol) and 2-pyridylmethyl chloride hydrochloride (3.28 g, 0.02 mol) in an aqueous solution (20 ml) of KOH (1.12 g, 0.02 mol) added with stirring. After addition of 1.38 g (0.01 mol) of  $\text{K}_2\text{CO}_3$ , the resulting red solution was stirred at 80 °C for 18 h. The solvent was then removed at reduced pressure and 20 ml of methanol were added to the resulting dark purple residue. After filtration, the dark purple filtrate was concentrated at reduced pressure to precipitate the crude product which was recrystallised from ethanol to give the purple product (4.69 g, 78%).  $\delta_{\text{H}}$  ( $(\text{CD}_3)_2\text{SO}$ , 298 K) 4.08 (s, 2 H), 4.49 (s, 4 H), 7.23 (t, 1 H), 7.70 (d, 1 H),

7.74 (t, 1 H) and 8.51 (d, 1 H).  $\tilde{\nu}_{\text{max}}/\text{cm}^{-1}$  3058, 1621s, 1594, 1443s, 1382, 1274 and 743s.

*Bis(2-benzimidazolylmethyl)(2-pyridylmethyl)amine (L)*. An 200 ml solution of 6 M HCl containing dipotassium *N*-(2-pyridylmethyl)iminodiacetate (3.00 g, 0.01 mol) and *o*-phenylenediamine (2.16 g, 0.02 mol) was refluxed for 72 h. A spoonful of active carbon was added after lowering the temperature and the solution continually refluxed for 5 min. After being filtered, the solution was treated with an excess of  $\text{NH}_4\text{OH}$  to give a brown residue which was collected by filtration and dissolved in 40 ml of  $\text{CHCl}_3$ . After filtration, the solution was washed three times with 20 ml of 0.1 M NaOH solution. Then, the  $\text{CHCl}_3$  was removed at reduced pressure to afford a solid that was recrystallized from ethanol to give the pure product as a yellow solid (1.53 g, 42%). The IR, MS (FAB), elemental analysis and  $^1\text{H}$  NMR data were identical to those obtained by method 1.

#### Syntheses of complexes

$[\text{LnL}(\text{NO}_3)_3] \cdot \text{C}_2\text{H}_5\text{OH}$  (Ln = La, Sm, Eu, Gd, Tb or Tm). To a clear solution of L (0.018 g, 0.05 mmol) in ethanol (5 ml) was added  $\text{Ln}(\text{NO}_3)_3 \cdot 5\text{H}_2\text{O}$  (0.05 mmol) in 5 ml of ethanol. The resulting solution was left standing overnight at room temperature to afford a pale yellow solid which was filtered off, washed three times with ethanol and diethyl ether successively, and dried over  $\text{CaCl}_2$  for 1 day to give the product in 50–70% yield. Pale yellow single crystals were obtained by vapor-phase diffusion of diethyl ether into the ethanol solution.

$[\text{LnLCl}_3(\text{H}_2\text{O})] \cdot \text{C}_2\text{H}_5\text{OH}$  (Ln = La, Sm, Eu, Tb or Ho). In a similar method, a solution of  $\text{LnCl}_3 \cdot 6\text{H}_2\text{O}$  (0.05 mmol) in 5 ml of ethanol was added to L (0.018 g, 0.05 mmol) in ethanol (5 ml) and the mixture treated as above. The yield was in the range 40–70%. Pale yellow single crystals were obtained as above.

FAB MS, IR and elemental analysis data for all complexes are summarized in Table 1.

#### Photophysical studies

Absorption spectra were obtained on a SHIMADZU UV-2501PC spectrophotometer, emission and excitation spectra on a HITACHI 850 spectrometer. Fluorescence quantum yields were determined by using  $[\text{Ru}(\text{bipy})_3]\text{Cl}_2$  (bipy = 2,2'-bipyridine;  $\Phi = 0.028$  in water)<sup>24</sup> as standard for the  $\text{Eu}^{3+}$  complex, and quinine sulfate ( $\Phi = 0.546$  in 0.5 mol  $\text{dm}^{-3}$   $\text{H}_2\text{SO}_4$ )<sup>25</sup> for the  $\text{Tb}^{3+}$  complex. The luminescence decays were recorded using a pumped dye laser (Lambda Physics model FL2002) as the excitation source. The nominal pulse width and the line-width of the dye-laser output were 10 ns and 0.18  $\text{cm}^{-1}$ , respectively. The emission of a sample was collected by two lenses into a monochromator (WDG30), detected by a photomultiplier and processed by a Boxcar Average (EGG model 162) in line with a microcomputer. The number of co-ordinated solvent molecules ( $q$ ) for the  $\text{Eu}^{3+}$  and  $\text{Tb}^{3+}$  complexes was calculated from Horrocks equation  $q = n(\tau_{\text{H}}^{-1} - \tau_{\text{D}}^{-1})$  where  $\tau_{\text{H}}$  is the lifetime in the protonated solvent (water or  $\text{CH}_3\text{OH}$ ),  $\tau_{\text{D}}$  that in the corresponding deuterated solvent, and the value of  $n$  is 1.05 ( $\text{Eu}^{3+}$  in  $\text{H}_2\text{O}/\text{D}_2\text{O}$ ), 4.2 ( $\text{Tb}^{3+}$  in  $\text{H}_2\text{O}/\text{D}_2\text{O}$ ), 2.1 ( $\text{Eu}^{3+}$  in  $\text{CH}_3\text{OH}/\text{CD}_3\text{OD}$ ), or 8.4 ( $\text{Tb}^{3+}$  in  $\text{CH}_3\text{OH}/\text{CD}_3\text{OD}$ ).<sup>1</sup>

#### X-Ray crystallography

Details of crystallographic parameters, data collection and refinements are listed in Table 2. The coordinates of the non-hydrogen atoms were refined anisotropically, while hydrogen atoms were included in the calculation isotropically but not refined. The ethanol solvate molecules in complexes 1 and 2 exhibit disorder over two positions and were refined isotropically with half site occupancy. In 3 the two carbon atoms of the

**Table 1** Mass, elemental analytical, IR spectral and conductivity data for complexes

FAB MS, $m/z$	Elemental analyses (%) <sup>a</sup>			IR ( $\tilde{\nu}_{\max}/\text{cm}^{-1}$ )		$A_M^c/\Omega^{-1}\text{cm}^2\text{mol}^{-1}$	
	C	H	N	$\tilde{\nu}_{\text{C-N}}^b$	$\tilde{\nu}_{\text{N-O}}$		
L	369 [M + H] <sup>+</sup>	71.93(71.72)	5.48(5.47)	23.08(22.81)	(1622,1594)		
[LaL(NO <sub>3</sub> ) <sub>3</sub> ] $\cdot$ C <sub>2</sub> H <sub>5</sub> OH	[M – EtOH – NO <sub>3</sub> + H] <sup>+</sup>	38.63(38.99)	3.61(3.54)	17.21(17.05)	(1623,1610)	(1295,1463)	187.2
[SmL(NO <sub>3</sub> ) <sub>3</sub> ] $\cdot$ C <sub>2</sub> H <sub>5</sub> OH		38.12(38.39)	3.41(3.49)	17.47(16.79)	(1622,1605)	(1295,1458)	191.2
[EuL(NO <sub>3</sub> ) <sub>3</sub> ] $\cdot$ C <sub>2</sub> H <sub>5</sub> OH		38.59(38.31)	3.63(3.48)	16.92(16.75)	(1621,1605)	(1295,1458)	209.1
[GdL(NO <sub>3</sub> ) <sub>3</sub> ] $\cdot$ C <sub>2</sub> H <sub>5</sub> OH		38.06(38.04)	3.37(3.46)	16.57(16.64)	(1623,1609)	(1300,1475)	201.7
[TbL(NO <sub>3</sub> ) <sub>3</sub> ] $\cdot$ C <sub>2</sub> H <sub>5</sub> OH	653 [M – EtOH – NO <sub>3</sub> + 2H] <sup>+</sup>	37.58(37.96)	3.36(3.45)	16.13(16.60)	(1623,1608)	(1298,1470)	219.9
[TmL(NO <sub>3</sub> ) <sub>3</sub> ] $\cdot$ C <sub>2</sub> H <sub>5</sub> OH		37.74(37.46)	3.43(3.41)	16.20(16.38)			221.7
[LaLCl <sub>3</sub> (H <sub>2</sub> O)] $\cdot$ C <sub>2</sub> H <sub>5</sub> OH	577 [M – EtOH – H <sub>2</sub> O – Cl] <sup>+</sup>	41.84(42.53)	3.89(4.16)	12.35(12.40)	(1624,1609)		
[SmLCl <sub>3</sub> (H <sub>2</sub> O)] $\cdot$ C <sub>2</sub> H <sub>5</sub> OH		41.85(41.82)	4.37(4.09)	12.09(12.19)	(1622,1609)		
[EuLCl <sub>3</sub> (H <sub>2</sub> O)] $\cdot$ C <sub>2</sub> H <sub>5</sub> OH	591 [M – EtOH – H <sub>2</sub> O – Cl + H] <sup>+</sup>	41.98(41.73)	3.95(4.08)	12.14(12.16)	(1623,1607)		
[TbLCl <sub>3</sub> (H <sub>2</sub> O)] $\cdot$ C <sub>2</sub> H <sub>5</sub> OH		41.58(41.31)	3.83(4.04)	12.31(12.04)	(1623,1606)		
[HoLCl <sub>3</sub> (H <sub>2</sub> O)] $\cdot$ C <sub>2</sub> H <sub>5</sub> OH		41.22(40.96)	4.36(4.01)	11.82(11.94)			

<sup>a</sup> Data in brackets are calculated values. <sup>b</sup> Imidazole ring. <sup>c</sup> Measured at 25 °C.

ethanol molecule were disordered between two slightly different locations with total occupancy of one, individually. Neutral atom scattering factors were taken from Cromer and Waber.<sup>26</sup>

CCDC reference number 186/2119.

See <http://www.rsc.org/suppdata/dt/b0/b003566l/> for crystallographic files in .cif format.

## Results and discussion

### Synthesis

Two different routes were designed to synthesize the ligand as shown in Scheme 1, using the same starting materials with reversed reaction processes and the final yields were quite different. In route 1, where condensation precedes substitution, although an excess of 2-pyridylmethyl chloride hydrochloride (**ii**) was used (**A** : **ii** = 1 : 2), the yield of the second step was quite low (15%) and 78% of bis(2-benzimidazolymethyl)amine was recovered at the end. It is possible that the steric hindrance resulting from free rotation of the two large benzimidazole groups prevents approach of the pyridylmethyl group. Change of the reaction conditions, *i.e.* the basicity of the reaction or the solvent, did not improve the yield. The yield of the first step was also not high (29%). In order to improve the total yield, route 2 was designed. The steric effect in the first step was small for the 2-pyridylmethyl group to react with the iminodiacetic acid and a good yield of **B** was obtained (78%). The final yield was 32% based on iminodiacetic acid, as compared to that of route 1, which was only 4%. Pure product was obtained after recrystallization and it was fairly soluble in many organic solvents such as methanol, acetone, acetonitrile and benzene.

In order to study how the anions control the reactions, both Ln(NO<sub>3</sub>)<sub>3</sub> and LnCl<sub>3</sub> were treated respectively with L in a 1 : 1 molar ratio in ethanol. Elemental analyses and FAB MS confirmed the 1 : 1 ligand : metal ratio for all complexes. On the basis of the similarity of their IR spectra (see later), it is assumed that the rest of the complexes have the same formula [LnL(NO<sub>3</sub>)<sub>3</sub>] $\cdot$ C<sub>2</sub>H<sub>5</sub>OH or [LnLCl<sub>3</sub>(H<sub>2</sub>O)] $\cdot$ C<sub>2</sub>H<sub>5</sub>OH (Table 1). In the FAB MS spectra of the complexes, besides the solvate ethanol molecule, some base ions lost one internal anion.

### Crystal structures

The crystallographic data for the complexes 1–3 are listed in Table 2 and their structures and atomic numbering schemes shown in Figs. 1, 2, and 3, respectively. Each complex is composed of a neutral [LnL(NO<sub>3</sub>)<sub>3</sub>] (Ln = Sm or Gd) or [SmLCl<sub>3</sub>(H<sub>2</sub>O)] entity and a solvated ethanol molecule. Complexes 1 and 2 are isomorphous with the central metal ion 10-coordinated, being linked to the four nitrogen atoms of the tetradentate ligand L and to the six oxygen atoms of three bidentate

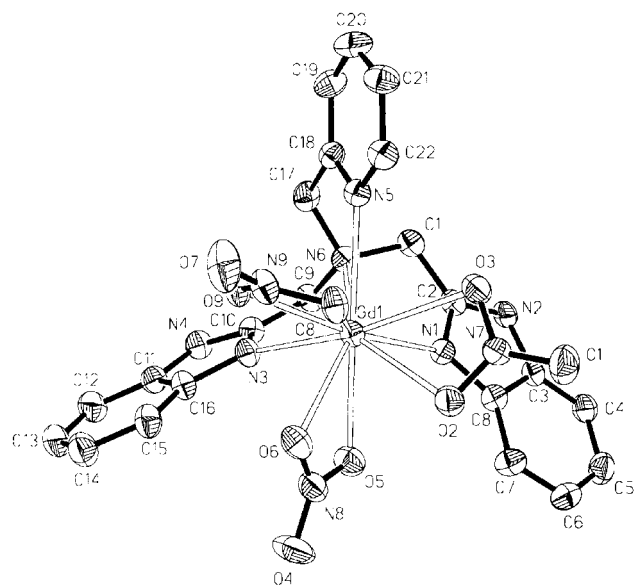


**Fig. 1** Molecular structure of the complex [GdL(NO<sub>3</sub>)<sub>3</sub>] $\cdot$ C<sub>2</sub>H<sub>5</sub>OH showing the atom labeling scheme. All hydrogen atoms have been omitted for clarity.

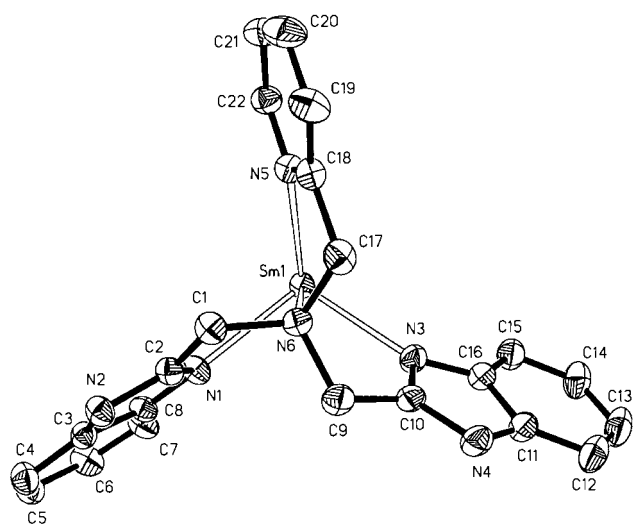
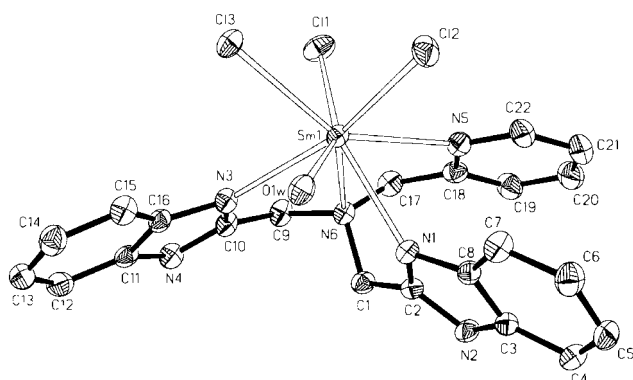
NO<sub>3</sub><sup>−</sup> groups. In the crystal structure of **3**, besides the four nitrogen atoms of the ligand and three chloride ions, there is one water molecule co-ordinated, resulting in an 8-co-ordinated metal ion. As mentioned earlier, nitrate-based lanthanide complexes have high co-ordination numbers as the donor atoms of bidentate nitrate are closer together than those of two independent monodentate ligands such as Cl<sup>−</sup>, due to the small bite angle in an NO<sub>3</sub><sup>−</sup> group.

For all the complexes, the ligand L exhibits a tripodal co-ordination mode, with three imino nitrogen (two from benzimidazolyl and one from pyridyl group) and one amino nitrogen atom as donors. Selected bond lengths are given in Table 3 (selected bond angles in Tables S1 and S2 in ESI). The average Ln–N<sub>imine</sub> distances (2.589 (**1**), 2.565 (**2**) and 2.620 (**3**) Å) are significantly shorter than Ln–N<sub>amine</sub> distances (2.725 (**1**), 2.696 (**2**) and 2.700 (**3**) Å), respectively, probably due to steric requirements. A similar phenomenon was reported for [Gd(L<sup>1</sup>)<sub>2</sub>] $\cdot$ (2CHCl<sub>3</sub>) (HL<sup>1</sup> = tris[2-(2-hydroxybenzylamino)ethyl]amine).<sup>16</sup> The average Ln–O distances in complexes **1** and **2** are 2.534 (**1**) and 2.512 (**2**) Å, respectively, comparable to those in the tripodal analogue [Ln(ntb)(NO<sub>3</sub>)<sub>2</sub>] $\cdot$ H<sub>2</sub>O (Ce–O 2.597, Er–O 2.473),<sup>21</sup> taking into account the difference in ionic radii.

It is interesting that the configuration of the ligand in complexes **1** and **2** is quite different from that in **3**. In the former the

**Table 2** Crystal data and structure refinement for complexes **1**, **2** and **3**

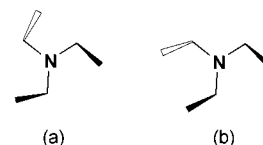
	<b>1</b>	<b>2</b>	<b>3</b>
Empirical formula	C <sub>24</sub> H <sub>26</sub> N <sub>9</sub> O <sub>10</sub> Sm	C <sub>24</sub> H <sub>26</sub> GdN <sub>9</sub> O <sub>10</sub>	C <sub>24</sub> H <sub>28</sub> Cl <sub>3</sub> N <sub>6</sub> O <sub>2</sub> Sm
Formula weight	750.89	757.79	689.22
Crystal system	Monoclinic	Monoclinic	Monoclinic
Space group	<i>P2<sub>1</sub>/c</i>	<i>P2<sub>1</sub>/c</i>	<i>P2<sub>1</sub>/c</i>
<i>a</i> /Å	10.3670(10)	10.3130(10)	11.6120(10)
<i>b</i> /Å	26.500(2)	26.376(2)	10.9130(10)
<i>c</i> /Å	11.4070(10)	11.3680(10)	21.5700(10)
$\beta$ /°	108.77	109.000(10)	100.19
<i>V</i> /Å <sup>3</sup>	2967.1(4)	2923.8(4)	2690.3(4)
<i>Z</i>	4	4	4
$\mu$ /mm <sup>-1</sup>	2.048	2.339	2.514
<i>T</i> /K	293(2)	293(2)	293(2)
<i>R</i> <sub>int</sub>	0.0329	0.0549	0.0318
No. reflections/observed	6424/4952	6372/4084	5870/4666
<i>R</i> 1 [ <i>I</i> > 2 $\sigma$ ( <i>I</i> )]	0.0343	0.0381	0.0241
<i>wR</i> 2 [ <i>I</i> > 2 $\sigma$ ( <i>I</i> )]	0.0834	0.0617	0.0489

**Fig. 2** View of the fan-like configuration of the ligand in [SmL-(NO<sub>3</sub>)<sub>3</sub>] $\cdot$ C<sub>2</sub>H<sub>5</sub>OH showing the atom labeling scheme. All hydrogen atoms and nitrate groups have been omitted for clarity.**Fig. 3** Molecular structure of the complex [SmLCl<sub>3</sub>(H<sub>2</sub>O)] $\cdot$ C<sub>2</sub>H<sub>5</sub>OH showing the atom labeling scheme. All hydrogen atoms have been omitted for clarity.

ligand exhibits a fan-like configuration (Scheme 2, a), with the three heterocyclic rings deflecting to the same direction and apart from each other at similar distances (Fig. 2). The distances between the centroids of the three rings are 6.808, 6.879, and 7.315 Å for complex **1** (or 6.783, 6.841, and 7.287 Å for **2**), and the angles N<sub>imine</sub>-Ln-N<sub>imine</sub> (99.43, 100.36, 102.66 (**1**) or 99.59, 100.47, 103.44° (**2**)) are also similar. However, in complex **3**, the pyridyl ring deflects to the opposite direction to the two benzimidazolyl rings, forming a pincer-like configuration

**Table 3** Selected bond lengths (Å) for complexes **1**, **2** and **3**

	<b>1</b>	<b>2</b>	<b>3</b>
M(1)-O(2)	2.491(3)	2.465(3)	
M(1)-O(3)	2.581(3)	2.558(3)	
M(1)-O(5)	2.549(3)	2.543(3)	
M(1)-O(6)	2.510(3)	2.482(3)	
M(1)-O(8)	2.511(3)	2.486(3)	
M(1)-O(9)	2.559(3)	2.537(3)	
M(1)-O(1W)			2.4943(18)
M(1)-Cl(1)			2.7055(7)
M(1)-Cl(2)			2.6967(7)
M(1)-Cl(3)			2.8184(7)
M(1)-N(1)	2.550(3)	2.531(3)	2.558(2)
M(1)-N(3)	2.547(3)	2.525(3)	2.575(2)
M(1)-N(5)	2.669(3)	2.640(4)	2.728(2)
M(1)-N(6)	2.725(3)	2.696(3)	2.700(2)

**Scheme 2** Fan-like (a) and pincer-like (b) configurations of the ligand (benzimidazolyl, —; pyridyl, —).

(Scheme 2, b). Consequently, the pyridyl ring inclines to the benzimidazolyl ring containing N(1), and the centroid-to-centroid distances (3.956, 7.100, 7.884 Å) and the N<sub>imine</sub>-Ln-N<sub>imine</sub> angles (64.46, 93.37, 127.15°) are quite different from each other (Fig. 3).

It is noteworthy that in complex **3** the dihedral angle between the pyridyl ring and the adjacent benzimidazolyl ring is 33.7°, together with the center-to-center distance of 3.96 Å, implying weak  $\pi$ - $\pi$  interaction between the two rings.<sup>27</sup> In the meantime, weak  $\pi$ - $\pi$  stacking interaction exists intermolecularly as shown in Fig. 4. The vertical distance between two offset benzimidazole rings which are exactly parallel is 3.53 Å. These intra- and inter-molecular interactions offset the steric effect of the two neighboring rings and stabilize the pincer-like configuration. On the other hand, as the pyridyl ring is close to one of the benzimidazole groups there is more space available to allow a water molecule to enter the co-ordination sphere. In complexes **1** and **2**, besides ligand L, the co-ordination environment of the metal ion is blocked by three bidentate nitrate ligands and a water molecule cannot enter the co-ordination cavity. Since co-ordinated solvent molecules, especially water or alcohol, can efficiently quench lanthanide luminescence, the ability to satisfy the co-ordination requirements of the lanthanide(III) centre with ten donors without additionally bound solvent molecules

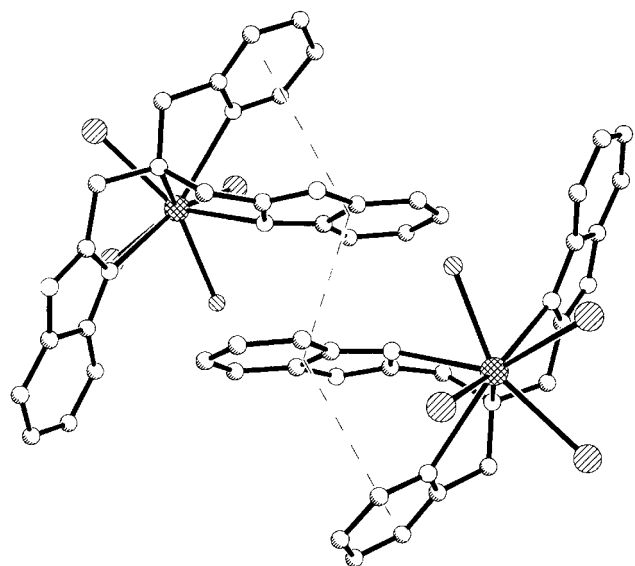


**Fig. 4** The intra- and inter-molecular  $\pi$ - $\pi$  stacking interactions between two molecules in the complex  $[\text{SmLCl}_3(\text{H}_2\text{O})]\cdot\text{C}_2\text{H}_5\text{OH}$ .

becomes an important criterion in the design of supra-molecular photonic devices.<sup>1</sup>

The hydrogen bonds play important roles in the crystal packing of all complexes. In **1** (or **2**), atoms O(7) and O(9) of one nitrate group act as hydrogen bond acceptors to form  $\text{O}\cdots\text{H}-\text{C}(12)$  ( $\text{O}\cdots\text{H}$ , 2.53 (**1**) and 2.57 Å (**2**),  $\text{O}\cdots\text{H}-\text{C}$ , 129.8 (**1**) and 129.9° (**2**)) and  $\text{O}\cdots\text{H}-\text{N}(4)$  ( $\text{O}\cdots\text{N}$ , 3.07 (**1**) and 3.07 Å (**2**),  $\text{O}\cdots\text{H}-\text{N}$ , 164.9 (**1**) and 166.7° (**2**)), respectively, with a neighboring molecule, where C(12) and N(4) are the hydrogen bond donors. In the mean time, O(1), O(3), C(4) and N(2) are involved in a cyclic hydrogen bonding mode with N(2), C(4), O(3) and O(1) atoms, respectively, of a third neighboring molecule ( $\text{O}\cdots\text{N}$ , 3.03 (**1**) and 3.04 Å (**2**),  $\text{O}\cdots\text{H}-\text{N}$ , 160.3 (**1**) and 159.8° (**2**);  $\text{O}\cdots\text{H}$ , 2.42 (**1**) and 2.43 Å (**2**),  $\text{O}\cdots\text{H}-\text{C}$ , 128 (**1**) and 127.6° (**2**)), thus generating a two-dimensional layer as shown in Fig. 5(a). In addition, such layers are cross-linked by  $\text{O}\cdots\text{H}-\text{C}$  ( $\text{O}\cdots\text{H}$ , 2.36 (**1**) and 2.37 Å (**2**),  $\text{O}\cdots\text{H}-\text{C}$ , 164.6 (**1**) and 166° (**2**)) formed between O(1) and C(6) belonging to adjacent layers, resulting in a three-dimensional open network (Fig. S1 in ESI). Extended channels are formed within the network along the *c* axis in which disordered ethanol molecules are accommodated. The ability of carbon atoms to act as proton donors in hydrogen bonds has been the subject of argument for many years and Taylor and Kennard<sup>28</sup> provided conclusive evidence of the existence of  $\text{C}-\text{H}\cdots\text{Y}$  ( $\text{Y} = \text{N}, \text{O}, \text{P}, \text{Cl}$  or  $\text{Br}$ ) in crystals in 1982. They showed that  $\text{C}-\text{H}\cdots\text{Y}$  contacts are electrostatic with the  $\text{C}-\text{H}-\text{Y}$  angle in the range of 90–180°, the distance between the donor and acceptor being shorter than the sum of their van der Waals radii. The  $\text{O}\cdots\text{H}$  distances found in **1** and **2** (2.36–2.58 Å) fall well within the estimated range of 2.16–2.65 Å.<sup>28</sup> Hydrogen bonding between aromatic hydrogen and electronegative atoms was also reported by Atwood *et al.*<sup>29</sup> The crystal packing in **3** is dominated by  $\text{Cl}\cdots\text{H}-\text{O}$  and  $\text{Cl}\cdots\text{H}-\text{N}$  hydrogen bondings. Each Cl(3) atom is connected to O(1w) ( $\text{Cl}\cdots\text{O}$  3.22 Å,  $\text{Cl}\cdots\text{H}-\text{O}$  141.8°) and N(4) ( $\text{Cl}\cdots\text{N}$  3.20 Å,  $\text{Cl}\cdots\text{H}-\text{N}$  151.6°) belonging to different molecules thus generating a two-dimensional layer as shown in Fig. 5(b). The crystal structure of **3** is stacked by such layers within which the disordered ethanol molecules are located.

### Infrared spectra

The “free” ligand exhibits two absorption bands at 1622 and 1594  $\text{cm}^{-1}$  which are assigned to the  $\text{C}=\text{N}$  stretchings in the imidazole ring.<sup>30</sup> The lanthanide complexes also exhibit these two bands. The high-energy band remains unchanged while the low-energy band blue shifts to about 1608  $\text{cm}^{-1}$  as compared to

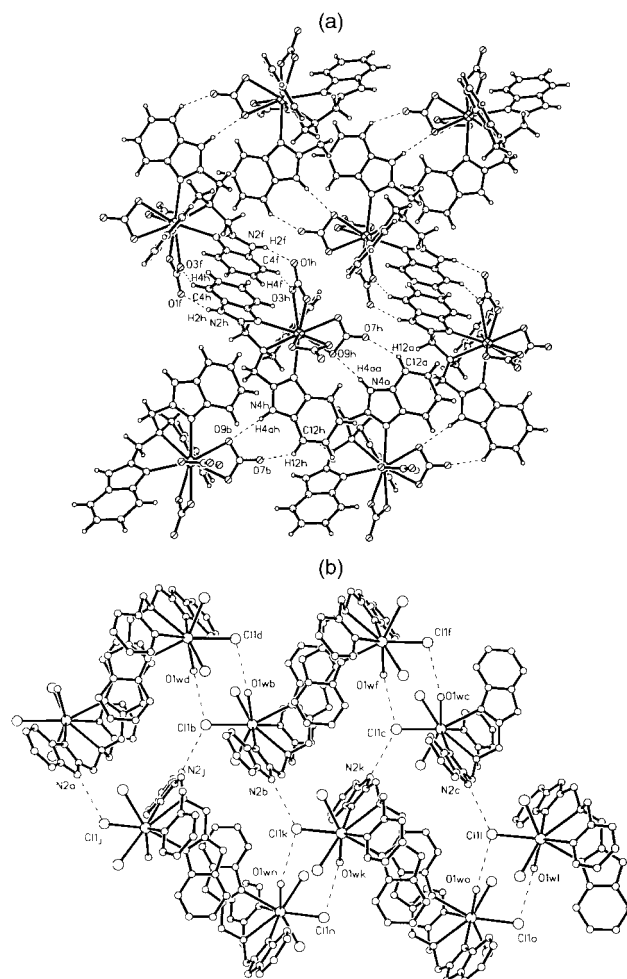


**Fig. 5** Hydrogen-bonding networks in the complexes: (a) 2-D layers generated by  $\text{O}\cdots\text{H}-\text{C}$  and  $\text{O}\cdots\text{H}-\text{N}$  hydrogen bonds in **1**; (b) 2-D layers generated by  $\text{Cl}\cdots\text{H}-\text{O}$  and  $\text{Cl}\cdots\text{H}-\text{N}$  hydrogen bonds in **3**.

its counterpart for the “free” ligand. For all the lanthanide complexes, broad bands at about 3450  $\text{cm}^{-1}$  occur from the O–H stretching vibrations of ethanol and water. In addition, the absence of bands at 1380, 820, and 720  $\text{cm}^{-1}$  in the spectra of  $[\text{LnL}(\text{NO}_3)_3]\cdot\text{C}_2\text{H}_5\text{OH}$  indicates that free nitrate groups ( $D_{3h}$ ) are absent, instead two intense absorptions associated with the asymmetric stretching appear in the ranges 1295–1300 ( $\nu_4$ ) and 1458–1475 ( $\nu_1$ )  $\text{cm}^{-1}$ , clearly establishing that the  $\text{NO}_3^-$  groups ( $C_{2v}$ ) are co-ordinated.<sup>31</sup> This is in agreement with the results of the structural analyses discussed above. The close similarity of the infrared spectra within each series  $[\text{LnL}(\text{NO}_3)_3]\cdot\text{C}_2\text{H}_5\text{OH}$  and  $[\text{LnLCl}_3(\text{H}_2\text{O})]\cdot\text{C}_2\text{H}_5\text{OH}$  suggests the same co-ordination behaviors in the respective complexes.

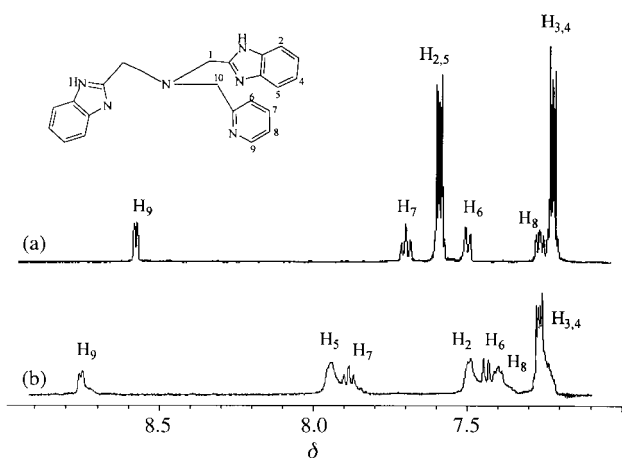
### <sup>1</sup>H NMR and conductivity studies in solution

The <sup>1</sup>H NMR spectra of the “free” ligand L and the diamagnetic lanthanum(III) complex  $[\text{LaL}(\text{NO}_3)_3]\cdot\text{C}_2\text{H}_5\text{OH}$  were measured in  $\text{CD}_3\text{CN}$  and  $\text{DMSO}-d_6$ . The chemical shift data are given in Table 4 and <sup>1</sup>H NMR spectra shown in Fig. 6. In  $\text{CD}_3\text{CN}$ , due to the electronic delocalization in imidazole rings and free rotation of the three arms, H<sup>2</sup> and H<sup>5</sup> in the “free” ligand have the same environments and show one signal ( $\delta$  7.59). However, the three arms of the ligand become more rigid after co-ordination in complex  $[\text{LaL}(\text{NO}_3)_3]\cdot\text{C}_2\text{H}_5\text{OH}$  and will be influenced by the co-ordinated N<sup>1</sup> and N<sup>3</sup> which become more electropositive, and the resonance of H<sup>5</sup> shifts to lower field ( $\delta$  7.95), as compared to that of H<sup>2</sup> ( $\delta$  7.50) which is farther away from N<sup>1</sup> and N<sup>3</sup>. For the four H<sup>3</sup> and H<sup>4</sup> hydrogens, the effect of the co-ordinated N<sup>1</sup> and N<sup>3</sup> nitrogen atoms becomes weaker and cannot be differentiated on the NMR timescale. In

**Table 4**  $^1\text{H}$  NMR data for the ligand and complex  $[\text{LaL}(\text{NO}_3)_3]\cdot\text{C}_2\text{H}_5\text{OH}$  in  $\text{CD}_3\text{CN}$  and  $\text{DMSO}-d_6$  (m, multiplet; s, singlet; d, double; t, triplet)

Compounds	$\delta_{\text{H10}}$	$\delta_{\text{H1}}$	$\delta_{\text{H3,4}}$	$\delta_{\text{H8}}$	$\delta_{\text{H6}}$	$\delta_{\text{H2,5}}$	$\delta_{\text{H7}}$	$\delta_{\text{H9}}$
L <sup>a</sup>	3.91 (s)	4.03 (s)	7.20 (m)	7.25 (t)	7.48 (d)	7.59 (m)	7.69 (t)	8.61 (d)
$[\text{LaL}(\text{NO}_3)_3]\cdot\text{C}_2\text{H}_5\text{OH}$ <sup>a</sup>	4.28 (m)	4.31 (d)	7.28 (m)	7.41 (t)	7.45 (d)	(7.50m, 7.95m)	7.89 (t)	8.75 (d)
L <sup>b</sup>	3.92 (s)	4.06 (s)	7.17 (m)	7.26 (dd)	7.70 (d)	7.57 (m)	7.77 (td)	8.52 (d)
$[\text{LaL}(\text{NO}_3)_3]\cdot\text{C}_2\text{H}_5\text{OH}$ <sup>b</sup>	3.95 (s)	4.07 (s)	7.16 (m)	7.24 (dd)	7.61 (d)	7.55 (m)	7.75 (td)	8.52 (d)

<sup>a</sup> Measured in  $\text{CD}_3\text{CN}$ . <sup>b</sup> Measured in  $\text{DMSO}-d_6$ .

**Fig. 6**  $^1\text{H}$  NMR spectra of the ligand L (a) and  $[\text{LaL}(\text{NO}_3)_3]\cdot\text{C}_2\text{H}_5\text{OH}$  (b) at 25 °C in  $\text{CD}_3\text{CN}$ .

$\text{DMSO}-d_6$  the complex  $[\text{LaL}(\text{NO}_3)_3]\cdot\text{C}_2\text{H}_5\text{OH}$  shows an identical  $^1\text{H}$  NMR spectrum to that of the “free” ligand, indicating that the ligand L has dissociated (Fig. S2 in ESI). Owing to the solvent effect, the  $^1\text{H}$  NMR spectrum of free L in  $\text{CD}_3\text{CN}$  is slightly different from that in  $\text{DMSO}-d_6$ .

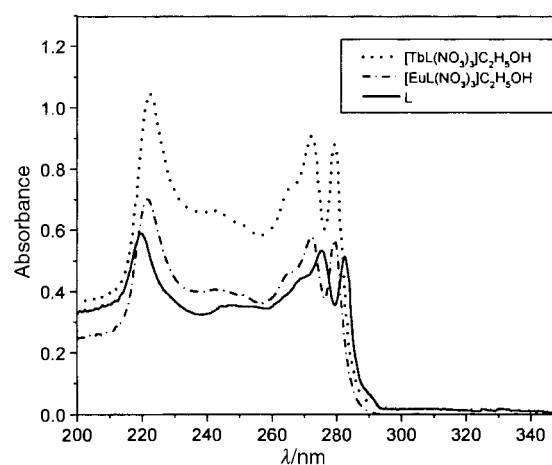
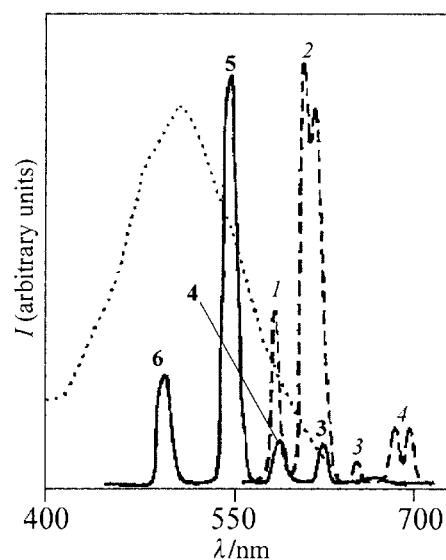
The conductivities of the complexes  $[\text{LaL}(\text{NO}_3)_3]\cdot\text{C}_2\text{H}_5\text{OH}$  were measured in  $\text{CH}_3\text{OH}$  and  $\text{CH}_3\text{CN}$ . The molar conductivities in  $\text{CH}_3\text{OH}$  lie in the range  $180\text{--}230\ \Omega^{-1}\ \text{cm}^2\ \text{mol}^{-1}$  (Table 1), indicating that all complexes are 2 : 1 electrolytes.<sup>32</sup> However, in  $\text{CH}_3\text{CN}$ , the molar conductances of these complexes are much smaller ( $\approx 100$  times) than those in methanol, indicating that the complexes remain intact and therefore neutral.

From the results of  $^1\text{H}$  NMR and conductivity measurements, it is seen that, in  $\delta$ -donor solvents, there is likely competition between the solvent and the ligand for the lanthanide ion. In the strongly polar  $\text{DMSO}$  the complex tends to decompose to form solvated  $\text{Ln}^{3+}$  species,<sup>33</sup> while in the moderately polar  $\text{CH}_3\text{CN}$  the complexes remain intact. In  $\text{CH}_3\text{OH}$  the ligand still co-ordinates, although two nitrates dissociate. A similar phenomenon was found in heptadentate  $\text{N}_4\text{O}_3$  Schiff base and ntb lanthanide complexes.<sup>15,20</sup>

#### Photophysical properties of the ligand and its $\text{Eu}^{3+}$ and $\text{Tb}^{3+}$ complexes

As the complexes are stable in  $\text{CH}_3\text{CN}$  the photophysical investigations were carried out in this solution. Free L displays three strong absorption bands in the UV spectral region at 220, 276 and 283 nm, arising from  $\pi\text{--}\pi^*$  transitions together with a broad low band around 245 nm (Fig. 7).<sup>34</sup> These bands are strongly perturbed upon co-ordination to  $\text{Ln}^{3+}$  in  $[\text{LnL}(\text{NO}_3)_3]\cdot\text{C}_2\text{H}_5\text{OH}$  and  $[\text{LnLCl}_3(\text{H}_2\text{O})]\cdot\text{C}_2\text{H}_5\text{OH}$  ( $\text{Ln} = \text{Eu}$  or  $\text{Tb}$ ) and blue shifts are found for the last two bands, implying co-ordination of the ligand. These complexes display almost identical spectral profiles and the absorption spectra of  $[\text{EuL}(\text{NO}_3)_3]\cdot\text{C}_2\text{H}_5\text{OH}$  and  $[\text{TbL}(\text{NO}_3)_3]\cdot\text{C}_2\text{H}_5\text{OH}$  are also shown in Fig. 7.

The luminescence spectra of the ligand and its  $\text{Eu}^{3+}$  and  $\text{Tb}^{3+}$  complexes were recorded at room temperature. Excited by the absorption band at 276 nm, the “free” ligand exhibits two broad emission bands ( $\lambda_{\text{max}} = 376$  and 504 nm) which may

**Fig. 7** Absorption spectra.**Fig. 8** The emission spectra of the ligand ( $\cdots$ ),  $[\text{EuL}(\text{NO}_3)_3]\cdot\text{C}_2\text{H}_5\text{OH}$  ( $-\ - -$ ;  $^5\text{D}_0 \rightarrow ^7\text{F}_J$ ,  $J = 1, 2, 3$  or  $4$ ) and  $[\text{TbL}(\text{NO}_3)_3]\cdot\text{C}_2\text{H}_5\text{OH}$  ( $—$ ;  $^5\text{D}_4 \rightarrow ^7\text{F}_J$ ,  $J = 3, 4, 5$  or  $6$ ).

correspond to the singlet and triplet states.<sup>3,18,35</sup> Excitations in the ligand-based  $\pi\text{--}\pi^*$  transitions cause the structured emission of lanthanide complexes while the ligand luminescence is completely quenched showing that ligand-to-metal energy transfer occurs.<sup>36</sup> The ability to transfer energy from ligand-centered to metal-centered is important in the design of lanthanide(III) supramolecular photonic devices.<sup>1,37</sup> The emission spectra of complexes  $[\text{EuL}(\text{NO}_3)_3]\cdot\text{C}_2\text{H}_5\text{OH}$  and  $[\text{TbL}(\text{NO}_3)_3]\cdot\text{C}_2\text{H}_5\text{OH}$  are shown in Fig. 8, and the emission quantum yields ( $\Phi$ ) are listed in Table 5. The stronger and better resolved spectrum of the  $\text{Tb}^{3+}$  complex ( $\Phi = 0.38$ ) showed the expected sequence of  $^5\text{D}_4 \rightarrow ^7\text{F}_J$  transitions ( $J = 6, 5, 4$  or  $3$ ) and no further splitting is visible due to the limitation of the equipment. In a typical spectrum ( $\Phi = 0.031$ , relatively weak) of the  $\text{Eu}^{3+}$  complex, the relative intensity of  $^5\text{D}_0 \rightarrow ^7\text{F}_2$  is more intense than that of  $^5\text{D}_0 \rightarrow ^7\text{F}_1$ , showing that the  $\text{Eu}^{3+}$  ion does not lie in a centrosymmetric co-ordination site.<sup>20</sup>

**Table 5** Luminescence lifetime data ( $\tau$ ) and derived solvation values ( $q$ ) for the  $\text{Eu}^{3+}$  and  $\text{Tb}^{3+}$  complexes

Complex	$\Phi$	$\tau/\text{ms}$				$q$	
		$\text{CH}_3\text{CN}$	$\text{CH}_3\text{OH}$	$\text{CD}_3\text{OD}$	$\text{CH}_3\text{CN}-\text{D}_2\text{O}$	water	$\text{CH}_3\text{OH}^b$
$[\text{EuL}(\text{NO}_3)_3]\cdot\text{C}_2\text{H}_5\text{OH}$	0.031	0.71	0.36	0.81	—	—	3.2
$[\text{TbL}(\text{NO}_3)_3]\cdot\text{C}_2\text{H}_5\text{OH}$	0.38	1.14	0.95	1.57	—	—	3.5
$[\text{EuLCl}_3(\text{H}_2\text{O})]\cdot\text{C}_2\text{H}_5\text{OH}$	0.001	0.31	—	—	0.25	0.8	—
$[\text{TbLCl}_3(\text{H}_2\text{O})]\cdot\text{C}_2\text{H}_5\text{OH}$	0.18	0.80	—	—	1.05	1.3	—

<sup>a</sup> The number of co-ordinated water molecules for complexes  $[\text{LnLCl}_3(\text{H}_2\text{O})]\cdot\text{C}_2\text{H}_5\text{OH}$  ( $\text{Ln} = \text{Eu}$  or  $\text{Tb}$ ) in  $\text{CH}_3\text{CN}$ . <sup>b</sup> The number of co-ordinated methanol molecules for complexes  $[\text{LnL}(\text{NO}_3)_3]\cdot\text{C}_2\text{H}_5\text{OH}$  ( $\text{Ln} = \text{Eu}$  or  $\text{Tb}$ ) in  $\text{CH}_3\text{OH}$ .

The values of  $\Phi$  for  $[\text{LnLCl}_3(\text{H}_2\text{O})]\cdot\text{C}_2\text{H}_5\text{OH}$  are lower than those for  $[\text{LnL}(\text{NO}_3)_3]\cdot\text{C}_2\text{H}_5\text{OH}$  ( $\text{Ln} = \text{Eu}$  or  $\text{Tb}$ ) which is evident from the fact that the co-ordinated water molecule in the former partially quenches the luminescence and decreases the  $\Phi$  value. Through vibronic coupling with the vibrational states of the O–H oscillators, efficient non-radiative deactivations take place in the lanthanide active state.<sup>37</sup> At the same time, by comparing the emission lifetimes of the complexes in  $\text{CH}_3\text{CN}$  before and after addition of a few drops of  $\text{D}_2\text{O}$  which will exchange with the water molecule, the effect of the co-ordinated water on the luminescence intensity of  $[\text{LnLCl}_3(\text{H}_2\text{O})]\cdot\text{C}_2\text{H}_5\text{OH}$  was checked.<sup>38</sup> The metal-centered emission lifetimes were determined by monitoring the decay of the  $^5\text{D}_0 \rightarrow ^7\text{F}_2$  transition (615 nm) for the  $\text{Eu}^{3+}$  complex, and the  $^5\text{D}_4 \rightarrow ^7\text{F}_5$  transition (550 nm) for the  $\text{Tb}^{3+}$  complex in  $\text{CH}_3\text{CN}$  and  $\text{CH}_3\text{CN}-\text{D}_2\text{O}$ . The lifetimes of metal-centered emissions become longer after treatment with  $\text{D}_2\text{O}$ , and use of the Horrocks equation gives the number of co-ordinated water molecules ( $q$ ) (see Table 5).<sup>1,37</sup> Considering the error in  $q$  ( $\pm 0.5$ ), the values of 0.8 for the  $\text{Eu}^{3+}$  complex and 1.3 for  $\text{Tb}^{3+}$  suggest one water molecule is co-ordinated in  $\text{CH}_3\text{CN}$ , in agreement with the crystallographic analyses.

The metal-centered emission lifetimes of  $[\text{LnL}(\text{NO}_3)_3]\cdot\text{C}_2\text{H}_5\text{OH}$  ( $\text{Ln} = \text{Eu}$  or  $\text{Tb}$ ) were determined in  $\text{CH}_3\text{CN}$ ,  $\text{CH}_3\text{OH}$  and  $\text{CD}_3\text{OD}$  (Table 5). The lifetimes in  $\text{CH}_3\text{CN}$  are considerably longer than in  $\text{CH}_3\text{OH}$ . As studied by  $^1\text{H}$  NMR and conductivity measurements, the nitrates do not dissociate in  $\text{CH}_3\text{CN}$ , so that solvent-based quenching is restricted to outer-sphere effects. However, two nitrates dissociate in  $\text{CH}_3\text{OH}$ , and methanol molecules, which can efficiently quench lanthanide luminescence, enter the co-ordination sphere. Calculated in the same way as above, the number of co-ordinated methanol molecules ( $q$ ) can be estimated by comparison of the luminescence lifetimes in  $\text{CH}_3\text{OH}$  and  $\text{CD}_3\text{OD}$ . Based on the greater quenching efficiency of the O–H group compared to the O–D group,<sup>1,37</sup> the lifetimes are longer in  $\text{CD}_3\text{OD}$  than in  $\text{CH}_3\text{OH}$ . The  $q$  values determined from these lifetimes are shown in Table 5. An average  $q$  of 3.4 suggests that there are three co-ordinated methanol molecules with an additional small contribution arising from outer-sphere solvation.<sup>39</sup> As a result, two nitrate groups are replaced by three methanol molecules forming  $[\text{LnL}(\text{NO}_3)(\text{CH}_3\text{OH})_3][\text{NO}_3]_2$  in which the central metal ion is 9-co-ordinated. These complexes are insoluble in water, so that it is not possible to compare the lifetimes in  $\text{D}_2\text{O}$  and water.

## Conclusion

With three arms suitably designed to absorb energy, the tripodal ligand bis(2-benzimidazolylmethyl)(2-*pridylmethyl*)-amine (**L**) is able to encapsulate a lanthanide ion to form an 1 : 1 complex. In the structures of complexes **1**, **2** and **3** two kinds of configuration (fan-like and pincer-like) for the ligand are found depending on the co-ordinating anions (anion controlled). Weak intra- and inter-molecular  $\pi-\pi$  interactions in **3** stabilize the pincer-like configuration. The complexes  $[\text{LnL}(\text{NO}_3)_3]\cdot\text{C}_2\text{H}_5\text{OH}$  dissociate in  $\text{CH}_3\text{OH}$  to give 2 : 1 electrolytes and luminescence lifetime studies when ( $\text{Ln} = \text{Eu}$  or  $\text{Tb}$ ) confirmed

the fact that dissociation of nitrates in methanol permits solvent-based quenching, with average effective solvation number ( $q$ ) of 3.4. In  $\text{CH}_3\text{CN}$  the emission quantum yields of  $[\text{LnL}(\text{NO}_3)_3]\cdot\text{C}_2\text{H}_5\text{OH}$  are higher than those of  $[\text{LnLCl}_3(\text{H}_2\text{O})]\cdot\text{C}_2\text{H}_5\text{OH}$  ( $\text{Ln} = \text{Eu}$  or  $\text{Tb}$ ) where there is one co-ordinated water molecule which could partially quench the luminescence.

## Acknowledgements

Financial support from the National Natural Science Foundation of China, the Natural Science Foundation of Guangdong Province and from the State Key Laboratory of Rare Earth Materials Chemistry and Applications, Peking University, is greatly appreciated.

## References

- N. Sabbatini, M. Guardigli and J. M. Lehn, *Coord. Chem. Rev.*, 1993, **123**, 201.
- C. Piguet, J.-C. G. Bünzli, G. Bernardinelli, G. Hopfgartner, S. Petoud and O. Schaad, *J. Am. Chem. Soc.*, 1996, **118**, 6681.
- C. Piguet, J.-C. G. Bünzli, G. Bernardinelli, G. Hopfgartner and A. F. Williams, *J. Am. Chem. Soc.*, 1993, **115**, 8197.
- E. Soini, I. Hemmila and P. Dhalen, *Ann. Biol. Chem.*, 1990, **48**, 567.
- J.-C. G. Bünzli, in *Lanthanide probes in Life, Chemical and Earth Sciences, Theory and Practice*, eds. J.-C. G. Bünzli and G. R. Choppin, Elsevier, New York, 1989, pp. 219–293.
- A. K. Saha, K. Kross, E. D. Kloszewski, D. A. Upson, J. L. Toner, R. A. Snow, C. D. V. Black and V. C. Desai, *J. Am. Chem. Soc.*, 1993, **115**, 11032.
- V. M. Mikkala, M. Heleniu, I. Hemmila, J. Kankare and H. Takalo, *Helv. Chim. Acta*, 1993, **76**, 1361.
- J.-M. Lehn and J.-B. Regnoul de Vains, *Helv. Chim. Acta*, 1992, **75**, 1221.
- V. M. Mikkala and J. J. Kankare, *Helv. Chim. Acta*, 1992, **75**, 1578.
- B. Alpha, J.-M. Lehn and G. Mathis, *Angew. Chem., Int. Ed. Engl.*, 1987, **26**, 266.
- V. Balzani, E. Berghmans, J.-M. Lehn, N. Sabbatini, A. Mecai, R. Therorde and R. Ziessel, *Helv. Chim. Acta*, 1990, **73**, 2083.
- D. Parker and J. A. Gareth Williams, *J. Chem. Soc., Dalton Trans.*, 1996, 3613.
- G. Mathis, *Clin. Chem.*, 1995, **41**, 1391.
- K. Kumar and M. F. Tweedle, *Pure Appl. Chem.*, 1993, **65**, 515.
- L.-W. Yang, S. Liu, E. Wong, S. J. Rettig and C. Orvig, *Inorg. Chem.*, 1995, **34**, 2164.
- S. Liu, L. Getmini, A. J. Remg, R. C. Thompson and C. Orvig, *J. Am. Chem. Soc.*, 1992, **114**, 6081.
- S. J. Archibald, A. J. Blake, S. Parsons, M. Schröder and R. E. P. Winpenny, *J. Chem. Soc., Dalton Trans.*, 1997, 173.
- C. Piguet, A. F. Williams, G. Bernardinelli and J.-C. G. Bünzli, *Inorg. Chem.*, 1993, **32**, 4139.
- R. Wietzka, M. Mazzanti, J.-M. Latour and J. Pécaut, *Chem. Commun.*, 1999, 209.
- C.-Y. Su, B.-S. Kang, X.-Q. Mu, J. Sun, Y.-X. Tong and Z.-N. Chen, *Aust. J. Chem.*, 1998, **51**, 565.
- C.-Y. Su, B.-S. Kang, H.-Q. Liu, Q.-G. Wang and T. C. W. Mak, *Chem. Commun.*, 1998, 1551.
- C.-Y. Su, B.-S. Kang, H.-Q. Liu, Q.-G. Wang, Z.-N. Chen, Z.-N. Lu, Y.-X. Tong and T. C. W. Mak, *Inorg. Chem.*, 1999, **38**, 1374.
- H. P. Berends and D. W. Stephan, *Inorg. Chim. Acta*, 1984, **93**, 173.
- K. Nakamaru, *Bull. Soc. Chem. Jpn.*, 1982, **5**, 2697.
- S. R. Meech and D. J. Philips, *J. Photochem.*, 1983, **23**, 193.

- 26 D. T. Cromer and J. T. Waber, *International Tables for X-Ray Crystallography*, Kynoch Press, Birmingham, 1974, vol. 4, Table 2.2A.
- 27 C. Piguet, J.-C. G. Bünzli, G. Bernardinelli, G. Hopfgartner and A. F. Williams, *J. Am. Chem. Soc.*, 1993, **115**, 8201.
- 28 R. Taylor and O. Kennard, *J. Am. Chem. Soc.*, 1982, **104**, 5063; G. A. Jeffrey and H. Maluszynska, *Int. J. Bio. Macromol.*, 1982, **4**, 173.
- 29 J. A. Atwood, F. Hamada, K. D. Robinson, G. W. Orr and R. L. Vincent, *Nature (London)*, 1991, **349**, 683.
- 30 L. K. Thompson, B. S. Ramaswamy and E. A. Seymour, *Can. J. Chem.*, 1997, **55**, 880.
- 31 W. T. Carnall, S. Siegel, J. K. Ferrano, B. Tani and E. Gebert, *Inorg. Chem.*, 1973, **12**, 560.
- 32 W. J. Geary, *Coord. Chem. Rev.*, 1971, **7**, 81.
- 33 J. V. Dagdigiam, V. Mckee and C. H. Reed, *Inorg. Chem.*, 1982, **21**, 1332.
- 34 C. Piguet, A. F. Williams, G. Bernardinelli, E. Moret and J. C. G. Bünzli, *Helv. Chim. Acta*, 1992, **75**, 1697.
- 35 C. Piguet, J.-C. G. Bünzli, G. Bernardinelli, C. G. Bochet and P. Froidevaux, *J. Chem. Soc., Dalton Trans.*, 1995, 83.
- 36 C. Piguet, G. Hopfgartner, A. F. Williams and J.-C. G. Bünzli, *J. Chem. Soc., Chem. Commun.*, 1995, 491.
- 37 W. D. Horrocks and D. R. Sudnick, *Acc. Chem. Res.*, 1981, **14**, 384.
- 38 Z. R. Reeves, K. L. V. Mann, J. C. Jeffery, J. A. M. Cleverty, M. D. Ward, F. Barigelletti and N. Armaroi, *J. Chem. Soc., Dalton Trans.*, 1999, 349.
- 39 S. Aime, M. Botta, D. Parker and J. A. G. Williams, *J. Chem. Soc., Dalton Trans.*, 1996, 17.